A FEASIBILITY ANALYSIS FOR THE DEVELOPMENT OF NOVEL AIRCRAFT WEIGHT AND BALANCE MONITORING SYSTEMS BASED ON FIBER BRAGG GRATING SENSORS TECHNOLOGY

Antonio IELE[1], Marco LEONE[1], Raffaella SOLIMENO[1], Carmine GRASSO[1], Giovanni Vito PERSIANO[1], Antonello CUTOLO[1], Marco CONSALES[1], Andrea CUSANO[1]

[1] Optoelectronics Group, Department of Engineering, University of Sannio, C.so Garibaldi 107, 82100 - Benevento (Italy)
a.iele@unisannio.it; marco.leone@unisannio.it; rmsolimeno88@gmail.com; cgrasso@unisannio.it; persiano@unisannio.it; cutolo@unisannio.it; consales@unisannio.it; a.cusano@unisannio.it

Abstract

This paper deals with a feasibility study of a new conception aircraft weight and balance (W&B) measurement system to be installed on aircraft landing gears, totally based on Fiber Bragg Grating (FBG) sensor technology. The basic idea relies on the determination of the instantaneous values of the weight and centre of gravity (CoG) coordinates of an aircraft by measuring, through the suitable combination of strain data provided by a FBG sensors network, the loads applied to the main/nose landing gears. To validate this system at the preliminary stage, we have designed and developed a lab mock-up demonstrator consisting of a metal plate (mimicking the aircraft body) supported by 3 PVC cylinders (simulating the landing gears), each one integrated with a FBG strain sensor. An extensive experimental analysis has been carried out by applying known weights to the plate placed at given coordinates, and then retrieving every value of weight and CoG from the strain data provided by the FBGs, once temperature effects are eliminated. Results obtained are in good agreement with those calculated with a suitably developed mathematical model, and demonstrate the capability of the proposed W&B architecture to determine the weight applied to the Lab mock-up with an accuracy <2%,as well as the CoG coordinates with millimetric precision.

Keywords: Fiber Optic Sensor, Fiber Bragg Gratings, Weight and Balance Measurement System, Center of Gravity, Airplane Landing Gear Monitoring

1 INTRODUCTION

It is well known that weight and location of CoG greatly affects the static and dynamic characteristics of airplanes and determine its safe operation [1]. Sufficiently accurate estimation of the gross weight and barycentre location can substantially improve overall performance of the air vehicle as these feedback signals can be put to good use within a condition based maintenance system, a health and usage monitoring system and the automatic flight control system [1]. The aircraft W&B estimation requires the calculation of the total weight of the airplane inclusive of passengers, fuel and baggage, and their location to obtain the perfect positioning of CoG. The safety and the stability of the aircraft can be compromised by wrong values of W&B as well as the fuel consumption and gas emission are not efficient. Currently, the estimations of the weight and balance are very inaccurate: indeed

the procedure consists of assigning to each passenger the same weight (hand baggage included) and placing baggage in a dedicated compartment at the after-body zone of the airplane. This procedure can generate errors that may lead to inconveniences, delays of flights and additional costs. So far, only a few approaches have been reported in literature for the CoG or W&B estimation, either numerical or experimental, all based on conventional technologies [2,3,4,5,6].
However, so far no works on the use of fiber optic sensors for the W&B determination have been reported in literature. FBG optical strain sensors are able to provide many advantages over conventional electrical systems particularly in applications require long-range and long-term deployments [7,8]. FBG optical sensing systems do not use electrical conductors and are therefore completely immune to EMI and high voltages. Open-air and harsh environments can also greatly benefit from optical sensing due to its immunity to lightning and resistance to metallic corrosion, potentially reducing the long-term maintenance costs of the system. In addition, dozens of FBG sensors, including temperature, strain, and pressure, can be written on the same optical fiber, and several hundreds of them can be simultaneously interrogated by one multi-channel interrogator.
Here, we report for the first time on a feasibility study of a new conception W&B measurement system, which is based on Fiber Bragg Grating (FBG) sensor technology and can be suitably installed on the aircraft landing gears for the determination of true weight and baricenter values of the aircraft during the taxing phase. The basic idea relies on the possibility to determine the instantaneous values of the aircraft weight and CoG coordinates, by retrieving (continuously and in real-time) the load distributions applied to the main and nose landing gears. These, in turn, can be carried out by the suitable correlation of strain measurements returned by the FBGs sensor network, suitably installed on the landing gear system. To preliminary validate the proof of principle, we have designed and developed an experimental lab mock-up consisting of a metal plate (mimicking the aircraft body) supported by 3 PVC cylinders (simulating the landing gears), each one integrated with a FBG strain sensor. Tests have been performed by applying known weights to the plate, in different points with known coordinates, and retrieving each time the weight and CoG of the system on the basis of the temperature corrected strain data provided by the FBGs.

2 EXPERIMENTALS

2.1 Lab mock-up

Figure 1 shows a schematic representation of the Lab mock-up used to experimentally demonstrate the proof of principle of the proposed W&B measurement system. The mock-up basically relies on an adjustable three-legged stand made of a 50cm x 50cm aluminium rigid plate (mimicking the aircraft body), supported by three PVC cylinders (simulating the three landing gears). The plate has been chosen sufficiently thick (2 cm) in order to safely assume it as not deformable. Each PVC cylinder has a diameter of 6 cm and a height of 15cm, and is fixed to the lower side of the plate through suitable metallic screws. The cylinders are positioned on the ground through metallic self-levelling legs, equipped with special screws that enable to finely adjust the height of each cylinder. The cylinder named as "C" simulates the nose landing gear, whereas cylinders "A" and "B" simulate the main ones.

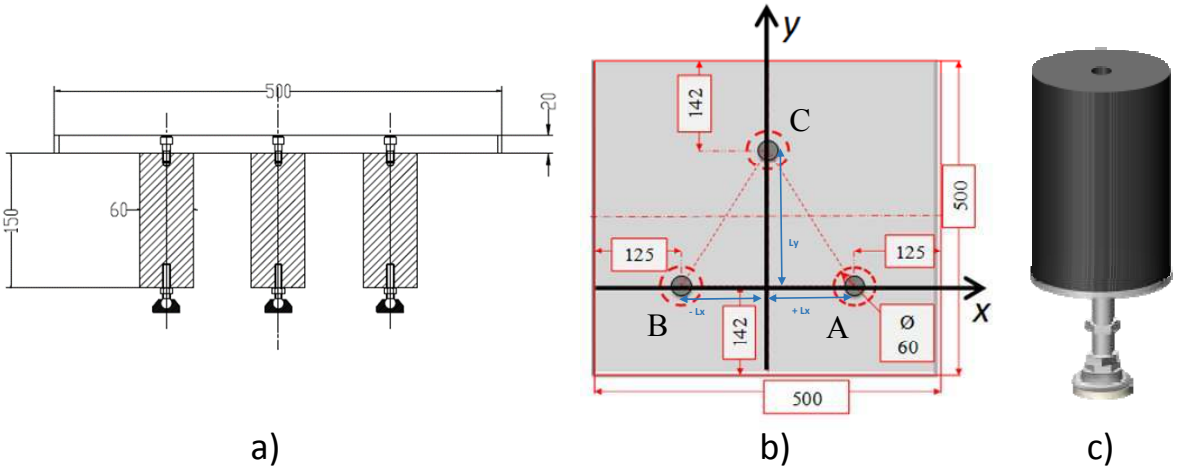

Figure 1: (a) Schematic representation of the mock-up structure; (b) drawing of the metal plate and (c) schematic representation of the PVC cylinders.

With reference to Fig 1.b, we know that just placing a mass M on the aluminium plate and also varying its (x,y) position results in changing the location of the mock-up barycentre. The deformation induced on each PVC support by the application/movement of the mass M can be monitored by a suitable strain sensors system, which allows to retrieve the force acting on each support and, hence, the weight of M. As the geometrical configuration of the three mounts and the force acting on each support are given, we are also able to deduce the CoG.
As robust and effective strain sensors for the precise determination of deformations induced to the three supports, we used fully polyimide recoated FBGs (5-mm long) suitably bonded to the lateral surface of each PVC support (namely "A", "B" and "C"). Specifically, after the preparation and cleaning of each PVC cylinders, the FBGs (one for each cylinder) were glued in the middle of the cylinder surface using standard cyanoacrylate glue. A controlled pre-strain was applied before gluing to each FBG to optimize their sensing performance. Finally, the cylinder was left under pressure for 24 hours to complete the bonding process.

2.2 FBGs as strain sensors

An FBG relies on a periodic modulation of the refractive index in the core of a single mode optical fiber. It behaves as a wavelength selective filter which reflects light signals at a specific wavelength, named the Bragg wavelength (λ_B), that is strictly dependent on the fiber effective refractive index (n_{eff}) and the grating pitch (Λ) of the FBG [7]:

$$\lambda_B = 2n_{eff}\Lambda \tag{1}$$

Both the refractive index and the grating pitch can be affected by strain and temperature, thus making FBGs very popular for strain and temperature sensing applications. [8-11]. Indeed, an axial strain in the grating changes the grating spatial period, as well as the effective refractive index and results in a shift of the Bragg wavelength due to the elastic behavior and elasto-optic effect, respectively. Similarly, the change of ambient temperature induces a similar effect on the grating, due to the thermal expansion and the thermo-optic effect.
Consequently, the Bragg wavelength shift ($\Delta\lambda_B$) due to the change in strain (ε) and temperature (ΔT) can be expressed as follows:

$$\Delta\lambda_B / \lambda_B = (1-P_e)\varepsilon + [(1-P_e)\alpha + \zeta]\Delta T \tag{2}$$

where Pe is the photo elastic-constant of the fiber, α is the thermal-expansion coefficient and ζ is the thermo-optic coefficient of the fiber. As the grating is intrinsically sensitive to both temperature variations and strain, the application of proper methods to decouple the effect of temperature and strain on the FBG readings needs to be foreseen in order to get precise strain measurements. This is what is generally referred to as temperature compensation [8].

2.3 Experimental setup

In our study, in order to obtain a temperature reference and compensate the thermal effects from the FBG strain sensors responses, a further FBG (equal to the other ones) has been glued on the lateral surface of an additional PVC cylinder (named as "T" in figure 2). The "T" cylinder is similar to cylinders A, B and C, but it is not screwed to the metal plate in such a way to be sensitive solely to temperature variation within the considered environment. The W&B measurement system is therefore made of three FBG strain sensors (bonded to cylinders A, B and C) and one temperature FBG sensor (bonded to cylinder T). In this configuration, it is possible to remove any thermal effect on the strain sensor response of the FBG bonded to the supports ($\Delta\lambda_{i,}$ i=A, B, C) by simply subtracting the wavelength shift returned by the temperature reference sensor ($\Delta\lambda_T$). The temperature-free signal output related to each FBG strain sensors thus become:

$$\Delta\lambda^{\varepsilon}_{A,B,C} = \Delta\lambda_{A,B,C} - \Delta\lambda_T \tag{3}$$

For the interrogation of all FBGs, a compact and robust four channels commercial interrogation system has been used (Miron Optics sm125), characterized by a wavelength stability and accuracy of 1 pm, a dynamic range of 50dB and a scan frequency of 2 Hz. Figure 2 shows a schematic representation of the assessed experimental setup.

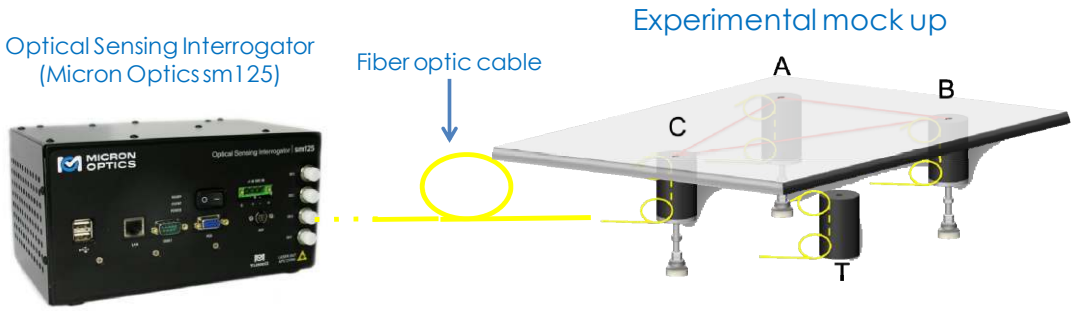

Figure 2: Experimental setup

3 MATHEMATICAL MODEL

In order to compare the results obtained by the experimental analysis with the theoretical ones, we also developed a proper mathematical model of the lab mock-up. The model enables to determine the precise weight and CoG position of the mock-up system on the basis of the forces applied on each cylinder due to the application/movement of the mass M upon the plate. It is based on the following assumptions:

- metal plate treated as a rigid body;

- PVC cylinders screwed in the metal plate and placed on the ground.

The interaction between the cylinders and the plate has been modelled by introducing 3 forces R_A, R_B, R_C, (reactions) directed along the vertical axes. The cylinder-plate system is placed on the ground with the cylinders transferring only normal forces (compression or traction). Moreover, assuming small displacements of the masses, the deviation of each cylinder axis from the vertical one and the plate rotation have been ignored.
Accordingly, in the most general case, the equilibrium conditions are represented by the following equations [12]:

- Vertical translational equilibrium:

$$R_A + R_B + R_C = P \tag{4}$$

- Rotational equilibrium around x:

$$R_A y_A + R_B y_B + R_C y_C = P\, y_G \tag{5}$$

- Rotational equilibrium around y:

$$R_A x_A + R_B x_B + R_C x_C = P\, x_G \tag{6}$$

where P is the total weight of the plate and the mass placed on it, x_i and y_i (i=A, B, C) are the coordinates of the cylinders A, B, C, x_g and y_g are the CoG coordinates of the whole system (i.e. plate + additional mass M). Relations (4), (5) and (6) can be used to obtain the reactions $R_{A,B,C}$ as a function of $x_{A,B,C}$, $y_{A,B,C}$, and x_g, y_g.
However, it is worth pointing out that, in our experiments, data returned by the FBG strain sensors (i.e. $\Delta\lambda_B$) are representative of the sole variations in the forces (reactions) acting on the three supports upon the application of the mass M (in the (x_M,y_M) position) with respect to an initial reference condition (i.e. relative to the unloaded plate). For this reason, the equilibrium forces in (4-6) represent variations of the reaction ΔR_i with respect to the reference one. Hence, the system reads:

$$\begin{cases} \Delta R_A + \Delta R_B + \Delta R_C = P_M \\ \Delta R_A y_A + \Delta R_B y_B + \Delta R_C y_C = P_M y_M \\ \Delta R_A x_A + \Delta R_B x_B + \Delta R_C x_C = P_M x_M \end{cases} \tag{7}$$

where P_M is the weight of the mass M, that, accordingly to the first equation of (7), can be retrieved by measuring the reaction variations on the three supports (A, B, C). Moreover, as shown in Fig 1.b, a reference system with the x-y plane coincident with the plate plane has been chosen. The points A, B, C form an equilateral triangle, with A and B being located on the x-axis ($y_A=y_B=0$ and $x_A= -x_B$) while C is on the y-axis ($x_C=0$). In particular, for the selected spatial reference system, the coordinates of the three cylinders are A=(Lx; 0), B=(-Lx; 0), C=(0; Ly). We can thus write:

$$\begin{cases} \Delta R_A = \dfrac{1}{2} P_M \left(1 - \dfrac{y_M}{Ly} + \dfrac{x_M}{Lx}\right) \\ \Delta R_B = \dfrac{1}{2} P_M \left(1 - \dfrac{y_M}{Ly} - \dfrac{x_M}{Lx}\right) \\ \Delta R_C = P_M \dfrac{y_M}{Ly} \end{cases} \tag{8}$$

Solving the system (8) with respect to x_M, y_M enables to derive also the position of the added mass M based on the ΔR_i:

$$\frac{y_M}{Ly} = \frac{\Delta R_C^M}{P_M}$$
$$\frac{x_M}{Lx} = \frac{\Delta R_A^M - \Delta R_B^M}{P_M} \tag{9}$$

Instead, the coordinates of the CoG can be written as follows [12]:

$$x_g = \frac{m_M}{m_M + m_p} x_M = K x_M \tag{10}$$

$$y_g = \frac{m_p}{m_M + m_p} y_{Gp} + \frac{m_M}{m_M + m_p} y_M = C + K y_M \tag{11}$$

$$\text{where } K = \frac{m_M}{m_M + m_p} \text{ and } C = \frac{m_p}{m_M + m_p} y_{Gp}$$

By combining (9), (10) and (11) we can finally obtain:

$$x_G = \frac{K}{P_M}\left(\Delta R_A - \Delta R_B\right) \cdot Lx$$
$$y_G = \left(C' + \frac{K}{P_M} \Delta R_C \right) \cdot Ly \tag{12}$$
$$\text{where } C' = \frac{C}{Ly}.$$

4 RESULTS AND DISCUSSIONS

In the most general case, when the plate is loaded with a mass M, each support experiences a certain force variation (ΔR_i) with respect to the unloaded condition, whose amplitude depends on the weight P_M and position (x_M, y_M) of the mass M. As a result, a correspondent blue wavelength shift is observed in the FBG strain sensors responses due to the compression of the cylinders to which they are bonded. If the mass is applied in correspondence of the point A (B or C), the force variation experienced by the cylinder A (B or C) is maximum (and equal to P_M), whereas those experienced by cylinders B and C is zero.

In light of these considerations, we first performed a calibration (in terms of $\Delta\lambda_i^{\varepsilon} - P_M$) of the FBG strain sensors bonded to the three supports, by placing known weights (21.4, 11.4 and 5.9 kg) onto the metal plate in correspondence of each cylinders. Test has been repeated five times for each sensor (and for each value of applied weight).

Fig. 3.a reports the output signals returned by the FBG strain sensors during the calibration tests. As expected, the $\Delta\lambda_i^{\varepsilon}$ provided by each strain sensor is zero when the mass is applied in correspondence of the other cylinders and increases with the weight of M when it is applied in correspondence of the cylinder to which they are bonded. In Fig. 3.b we show the experimentally obtained calibration curves ($\Delta\lambda_i^{\varepsilon} - P_M$) of the three strain sensors, all exhibiting a linear behaviour. By considering the slope of the linear fitting curves, the sensitivity of each

sensor vs. the applied weight can be obtained (they are reported in the insets of fig. 3.b). Such values are extremely important, as they can be used to retrieve, by means of the $\Delta\lambda_i^{\varepsilon}$ returned by the FBG strain sensors, the weight (force) acting on each support due to the application/movement of the mass M.

Once completed the calibration test, we successively carried out a deep experimental campaign by applying a known weight on the plate (in different positions along the x and y axes) and retrieving, on the basis of the FBG strain sensors responses and of the theoretical model described in section 3, the applied weight and the CoG coordinates of the mock-up.

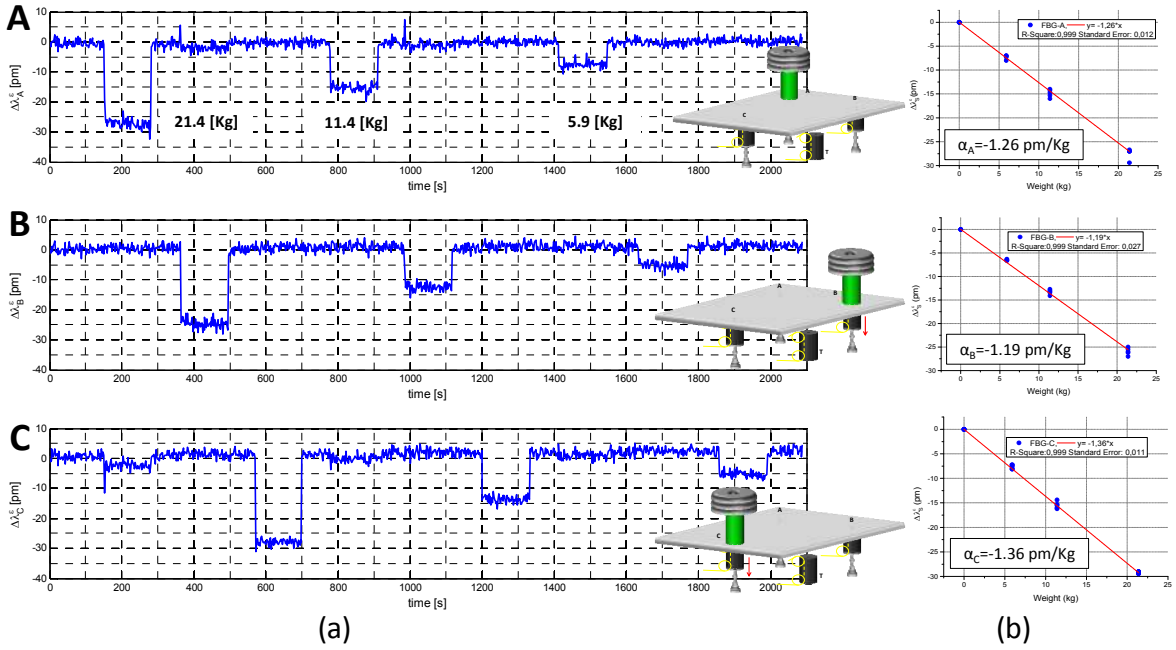

Figure 3: (a) FBG sensor responses during the calibration tests and (b) calibration curves of the three FBG strain sensors.

Fig. 4.a shows the output signals returned by the FBG strain sensors when the mass M (with weight 21.4 Kg) is moved along the x axis (y=0 and x= x_1, x_2, x_3, x_4, x_5), from position x1 (-125 mm, i.e. point B) to position x5 (125 mm, i.e. point A). As theoretically expected, $\Delta\lambda_C^{\varepsilon}$ is zero as all the forces result to be applied solely on cylinders A and B (located along the x axis). The response of sensor "B" ("A") is maximum in correspondence of x1 (x5), and gradually decreases by moving M toward position x5 (x1), in correspondence of which it is zero. In addition, when M is applied in position x3 (x=0; y=0) $\Delta\lambda_A^{\varepsilon} \approx \Delta\lambda_B^{\varepsilon}$.

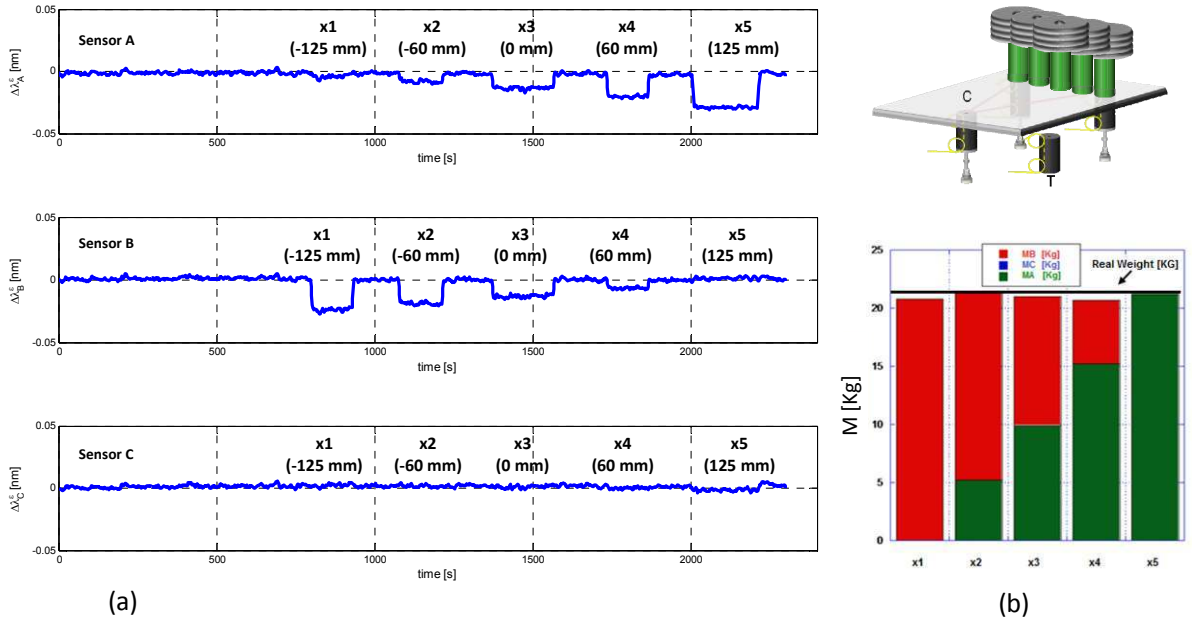

Figure 4: (a) FBG sensor responses during the tests along x axis and (b) estimated weights retrieved using the FBG strain sensors responses for all x positions.

Starting from the $\Delta\lambda_i^{\varepsilon}$ returned by each FBG strain sensor, and using the sensitivity coefficient α_i obtained during the calibration tests, the total applied weight can be reconstructed by summing the single force contributions observed on each support:

$$M = M_A + M_B + M_C \tag{13}$$

where

$$M_A = \frac{\Delta\lambda_A^{\varepsilon}}{\alpha_A},\ M_B = \frac{\Delta\lambda_B^{\varepsilon}}{\alpha_B} \text{ and } M_C = \frac{\Delta\lambda_C^{\varepsilon}}{\alpha_C} \tag{14}$$

The weights for all x positions in the histogram of Fig. 4.b show a very good agreement between estimated and real values. Indeed, the accuracy of the FBG sensors systems in weight estimation turned out to be less than 2%.
Similar results have also been obtained by applying the same mass M on the plate along the y axis (x=0 and y= y_1, y_2, y_3, y_4), from position y1 (0 mm) to the position y4 (216 mm, i.e. point C). The output signals returned by the FBG strain sensors and the histogram reporting the estimated weights for all y positions are shown in Fig. 5. Also in this case the system accuracy was estimated to be ~2%.

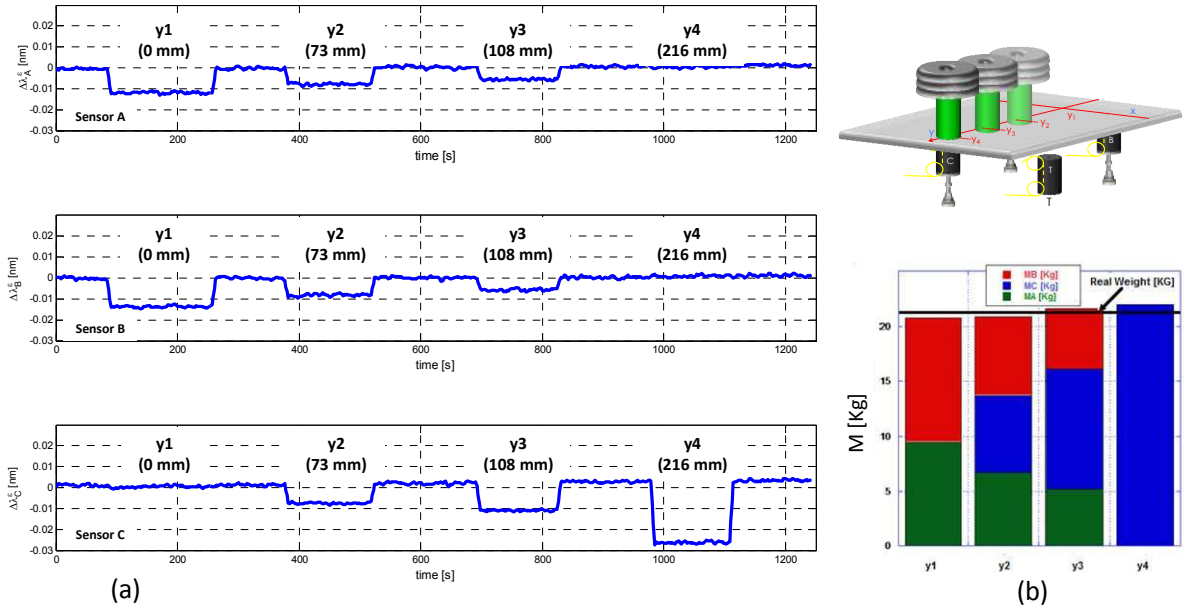

Figure 5: (a) FBG sensor responses during the tests along y axis and (b) estimated weights retrieved using the FBG strain sensors responses for all y positions.

In addition to the weight estimation pertaining to the mass applied onto the metal plate, the FBG strain sensor responses returned during the tests along x and y axes have also been used to retrieve, each time, the instantaneous position of the mock-up CoG (i.e. the instantaneous values of x_g, y_g). To achieve this aim, we used the theoretical model described in section 3.
In table 1 and 2 we resume the CoG coordinates obtained both experimentally (by feeding the developed model with the responses returned by each strain sensor) and theoretically (by feeding the same model with the real values) during the tests along the x and y axes, respectively. Both tables also report the error (in mm) made in the estimation of the CoG coordinates x_g and y_g. As evident, the maximum error turned out to be ~4mm and ~6mm, respectively during tests carried out along the x and y axis.

	CoG coordinates [mm]				Error [mm]	
	x_g exp	y_g exp	x_g theor	y_g theor	Δx_g	Δy_g
x_1	-72.6	45.2	-73.5	44.5	0.9	0.7
x_2	-37.4	44.5	-35.3	44.5	-2.1	0.0
x_3	-4.2	45.0	0.0	44.5	-4.2	0.5
x_4	33.9	45.2	35.3	44.5	-1.4	0.7
x_5	73.2	44.7	73.5	44.5	-0.3	0.2

Table 1

	CoG coordinates [mm]				Error [mm]	
	x_g exp	y_g exp	x_g theor	y_g theor	Δx_g	Δy_g
y_1	-6.3	45.1	0.0	44.5	-6.3	0.6
y_2	-1.7	87.0	0.0	87.4	-1.7	-0.4
y_3	-1.0	108.6	0.0	108.0	-1.0	0.6
y_4	0.0	172.2	0.0	171.5	0.0	0.7

Table 2

Table 1-2: CoG coordinates obtained both experimentally and theoretically during the tests along the x and y axes, respectively; the errors (calculated in mm) in the estimation of the CoG coordinates are also reported.

Overall, results here reported represents a clear demonstration of the capability of the developed fiber optic sensors system to accurately determine the instantaneous values of weight and CoG coordinates of the simplified lab mock-up system and paves the way to its future applications to real landing gears for the determination of real aircraft W&B during the taxis phase.

6 CONCLUSIONS

In this work we reported on the feasibility study of a novel aircraft weight and balance (W&B) measurement system, totally based on Fiber Bragg Grating (FBG) sensor technology, to be installed on aircraft landing gears. The basic idea relies on the possibility to determine the instantaneous values of the weight and CoG coordinates of an aircraft by continuously retrieving, through a suitable FBG strain sensor system, the distributions of forces (loads) applied to the main and nose landing gears. To preliminary validate the proof of principle, we designed and developed an experimental lab mock-up, able to mimicking the aircraft body and the main/nose landing gears, suitably integrated with a FBG strain sensor network. Results obtained from an extensive experimental campaign, performed by applying known weights to the mock-up (in different points with known coordinates) and by retrieving each time the weight and CoG of the system on the basis of the strain sensors response as well as of a suitably developed theoretical model, demonstrated the potentiality of the proposed W&B architecture and encourages its exploitation in concrete applications.

7 ACKNOWLEDGMENTS

The work is supported by the Italian Ministry of University and Research under the National Projects PON03PE_00135, "CAPRI - Carrello per Atterraggio con Attuazione Intelligente".

REFERENCES

[1] M. Abraham, M. Costello, In-Flight Estimation of Helicopter Gross Weight and Mass Center Location. *Journal of Aircraft*, **46**, 2009.

[2] M. F. Almalki, M. Elshafei, Method and apparatus for tracking center of gravity of air vehicle. *United States Patent Application Publication*, US 2009/0143926 A1, 2009.

[3] Y.M. Al-Rawashdeh, M. Elshafei, M.F. Al-Malki, In-Flight Estimation of Center of Gravity Position Using All-Accelerometers. *Sensors*, **14**, 17567-17585, 2014.

[4] J. Cummins, J.A. Bering, D.E. Adams, R. Sterkenburg, Automated estimation of an aircraft's center of gravity using static and dynamic measurements. *Proceedings of the IMAC-XXVII*, 2009.

[5] Federal Aviation Administration. "*Aircraft Weight and Balance Handbook: FAA-H-8083-1A",* Aviation Supplies and Academics (2007).

[6] D. Hughes, Crane Offers Aircraft Weight and Balance System, *Aviation Week & Space Technology*, **162**, 91, 2005.

[7] K.O. Hill, G. Meltz, Fiber Bragg grating technology fundamentals and overview. *Journal of lightwave technology,***15**, 1263–1276, 1997.

[8] Y.J. Rao, In-fibre Bragg grating sensors. *Measurement science and technology,* **8**, 355–375, 1997.

[9] A.D. Kersey, M.A. Davis, H.J. Patrick, M. LeBlanc, K.P. Koo, Fiber grating sensors. *Journal of lightwave technology,* **15**, 1442–1463, 1997.

[10] A. Cusano, A. Cutolo, J. Albert. *"Fiber Bragg grating sensors: recent advancements, industrial applications and market exploitation"*, Bentham Science Publishers ISBN: 978-1-60805-343-8 (2011).

[11] G. Berruti, M. Consales, M. Giordano, L. Sansone, P. Petagna, S. Buontempo, A. Cusano, Radiation hard humidity sensors for high energy physics applications using polyimide-coated fiber Bragg gratings sensors. *Sensors and Actuators B: Chemical*, **177**, 94-102, 2013.

[12] V. Franciosi, "*Lezioni di Scienza delle Costruzioni"*, vol. I, Liguori, Napoli (1959)